HHS Public Access

Author manuscript

Neurosurg Clin N Am. Author manuscript; available in PMC 2018 October 01.

Published in final edited form as:

Neurosurg Clin N Am. 2017 October ; 28(4): 499–512. doi:10.1016/j.nec.2017.05.005.

iMRI during transsphenoidal surgery (TSS)

Prashant Chittiboina, MD, MPH

Assistant Clinical Investigator, Neurosurgery Unit for Pituitary and Inheritable Diseases, National Institute of Neurological Diseases and Stroke, National Institutes of Health, 10 Center Drive, Room 3D20, Bethesda, MD 20892-1414

Abstract

Surgeons routinely use adjunct imaging tools during transsphenoidal surgery (TSS). Intra-operative MRI (iMRI) was quickly adopted as a surgical adjunct for TSS. Currently, a variety of iMRI systems are in use during TSS. The variations in iMRI systems include field strengths (0.15 to 3 T), magnet configurations (open, retractable, double doughnut etc.) and room configurations. Most studies report that the primary utility of iMRI during TSS lies in detecting resectable tumor residuals following maximal resection with conventional technique. Additionally, stereotaxis, neuronavigation and complication avoidance/detection are enhanced by iMRI use during TSS. The use of iMRI during TSS can lead to increased extent of resection for large tumors. Additionally, improved remission rates from hormone secreting tumors have also been reported with iMRI use. Despite increased surgical duration with iMRI, the incidence of surgical or peri-operative complications are comparable with conventional TSS. In this chapter, the history, indications and future directions for iMRI during TSS are discussed.

Keywords

interventional; intraoperative; MRI; iMRI; pituitary; adenoma; transsphenoidal

Introduction

Transsphenoidal surgery (TSS) has an important role in the management of pituitary tumors. For many tumors, including non-functioning pituitary adenomas (NFPA)[1], corticotrophin secreting adenomas (CA) causing Cushing's disease (CD)[2] and growth hormone secreting adenomas (GA) causing acromegaly[3], TSS remains the therapy of first choice. Medical management has replaced TSS as the therapy of first choice for one type of pituitary tumor – prolactinoma. For the rest of the tumor types, patients are first advised to undergo TSS.

First described in 1907 by Schloffer, TSS was later refined and popularized by Harvey Cushing.[4] Despite rapid refinements in the technique that allowed for reduction of mortality

Phone: (301) 496-5728, prashant.chittiboina@nih.gov.

Disclosure: The author has nothing to disclose.

rates to as low as 5.3% by 1925[5], the procedure was abandoned by Dr. Cushing. With improved visualization through the operating microscope, Jules Hardy, re-introduced TSS in the modern era, setting the stage for a later development of techniques necessary for selective removal of microadenomas (tumors smaller than 1 cm) and macroadenomas.[4] Today, the procedure is widely used, and is the technique of choice for resection of pituitary tumors. For patients undergoing TSS for pituitary tumors, remission rates vary. In a recent meta-analysis, the mean remission rates (ranges) were 68.8% (27–100) for prolactinomas, 47.3% (3–92) for NFA, 61.2% (37–88) for GA, and 71.3% (41–98) for CA tumors. Remission rates and incidence of recurrence have improved modestly over the past three decades.[6]

Currently, overcoming the following challenges could improve remission rates after pituitary surgery: 1. Visibility of small tumors: remission is dependent of the ability to detect the adenomas; 2. Visualization of true extent of large tumors: For larger tumors, cure rates are reduced by tumor remnants. 3. Visualization of tumor invasion: extension of tumor into the structures surrounding the sella. Technologies introduced to take on these challenges include endoscopy,[4] frameless stereotaxy,[7] color Doppler ultrasonography and real-time intraoperative MRI (iMRI).[8–11]

iMRI for TSS

History of Intraoperative Imaging during TSS

Surgeons routinely use adjunct imaging tools during transsphenoidal surgery. Popularized by Jules Hardy[12], intra-operative fluoroscopic imaging is widely used by surgeons to define the superior and inferior limits of the sella turcica.[13] Frameless stereotactic fluoroscopic guidance registers pre-operative CT or MRI images with intraoperative fluoroscopy.[14] This technique employs accurate stereotaxy to ensure that the surgical approach avoids injury to critical structures like the internal carotid arteries.[13] These stereotaxic techniques, however, are not useful for monitoring extent of resection (resection control) of pituitary macroadenomas. Intraoperative ultrasonography (iUSG), either by trans-cranial[15,16] or trans-sellar[17–19] routes provides imaging of sellar/supra-sellar contents in real time. Investigators have used iUSG to detect tumor residuals and critical structures like the carotid arteries.[17–19] In addition, iUSG has had some success in detecting microadenomas.[20,21] In patients with Cushing's disease with negative pre-operative imaging, iUSG detected up to 69% of micro-adenomas.[21] Despite significant advantages including ease of use, real-time imaging, low cost and lack of radiation, iUSG remains infrequently used during TSS due to poor image quality.[13]

History of iMRI for TSS

Interventions in the head and neck region within the MRI suite were initially limited to needle biopsies and aspirations.[22] The limitations were the product of conventional horizontal bore design of the MRI machines. Long acquisition times compared with other guidance methods including computed tomography (CT) or fluoroscopy made interventions in the MRI suite complicated and difficult to perform.[23] Another MRI configuration was needed to ensure ease of manipulation and surgical access. A midfield MRI system (Signa

SP, General Electric, Boston, MA) was conceptualized and installed at the Brigham and Women's Hospital in Boston in 1994 to address issues of surgical access.[24,25] It's 'double doughnut' configuration allowed real-time monitoring and complete access to the surgical site and an intra-operative MRI tracking system for real-time stereotaxy and neuronavigation. The surgeon accessed the patient's head and neck region between two large 'doughnuts' containing superconducting magnets. Although the surgical access was unparalleled among the iMRI system, the design was not widely replicated in other centers introducing iMRI systems. Another popular early design was the 'open' MRI configuration that allowed improved lateral access, but with restricted vertical access. The examples include the Toshiba Access (Toshiba America Medical Systems, Tustin, CA) in a 'temple' format, and the Magnetom Open (Siemens AG, Erlangen, Germany) in the 'C-arm' format in Erlangen, Germany.[23] These and the subsequent iterations of iMRI invoked the 'single room, moveable table' format that allowed surgery to be performed outside the 5-Gauss (G) line. Surgical procedures outside the 5-G line could be performed using the standard surgical instruments including the operating microscope, and patients could be moved quickly into the scanner for intra-operative imaging.[10] Initial reports of iMRI use for neurosurgical indications included TSS procedures.[10,26,27] Surgeons recognized the potential of iMRI for resection control of macroadenomas and for detection of intra-operative hematomas during TSS.[10,27] Other systems including the retractable ultra-low field strength (PoleStar N-10 and N-20, Odin Medical Technologies, Newton, MA)[28–30], low field strength moveable magnet (Hitachi AIRIS II, Hitachi Medical, Twinsburg, OH) [31], high-field moveable magnet (IMRIS, Marconi Medical System, Winnipeg, Ontario, Canada), and the 3 Tesla machines[32], have all been designed for optimal use of existing surgical tools and microscopes outside the 5-G line. The ability to use conventional tools likely reduces the barrier to introduction and adoption of iMRI procedures. Similarly, shared-resource strategies for utilizing the iMRI machine for both intra-operative imaging and routine diagnostic imaging are increasingly being adopted to offset initial investment costs.[31,33,34] Recently, most centers are re-introducing conventional horizontal bore machines with high (1.5 T) or ultra-high (3 T) field strength. Higher field strength improves image resolution and reduces image acquisition time, at the expense of surgical access during this period.

Types of iMRI systems

A variety of iMRI systems have been used during TSS (Table 1). The iMRI systems vary in field strengths (0.15 to 3 T), magnet configurations (open, retractable, double doughnut etc.) and room configurations. Most studies report that the primary benefit of iMRI during TSS lies in intraoperative detection of tumor residuals following maximal resection with conventional technique. Few studies compare the iMRI systems head-to-head to evaluate their comparative effectiveness in detecting tumor residuals.

Field Strength—First reports of TSS and iMRI described low field strength (0.2 – 0.5 T) systems.[10,27] These, and subsequent studies using low field strength magnets used post-contrast T1-weighted (T1W) images to detect adenoma as well as the normal pituitary gland.[10,31,35] Some studies used dynamic post-contrast studies as the primary sequence to differentiate normal pituitary gland from adenoma residuals.[26,27,36] Higher field strength magnets (1.5 T) demonstrated improved image resolution and decreased image acquisition

time, allowing for non-contrast T2-weighted (T2W) images to be performed as the primary sequence. Post-contrast T1W images were selectively applied to those tumors that enhanced with contrast pre-operatively.[37,38] With high-resolution T2W images possible in 3 T iMRI systems, it may be possible to avoid intra-operative contrast injection entirely.[34] In general, the rate of gross total resection (GTR) of pituitary adenomas reported in studies using low field strength (< 0.5 T) iMRIs ranged from 3% to 33%. Similarly, the rate of GTR ranged from 15 – 40% in studies with higher field (≥ 0.5 T) strength iMRI systems.[39] In a direct comparison of TSS procedures performed in 0.2 T iMRI vs. 1.5 T iMRI platforms within the same institution, the authors reported an increase in the number of patients undergoing re-exploration during the operative procedure (28.8% vs. 36.4%) with the high field strength system.[37] Better image resolution of suprasellar and parasellar structures likely underlies the advantage of higher field strength iMRI systems in improving the rate of GTR.

Magnet configuration—The 'double doughnut' configuration[26,27,36,40,41] (Signa SP, General Electric, Boston, MA) allowed 'live' interventional imaging of the surgical field during TSS. This allowed for real-time adjustment of the plane of approach to the sella.[26] Traditionally, surgeons have used video-flouroscopy[12] or neuro-navigation for this function.[13,14,42] Similar to the later iMRI practice, following the initial surgical approach, surgeons obtained images of the surgical field following maximal possible resection as assessed by direct visualization. Later iMRI magnet configurations typically require cessation of TSS procedure for the duration of image acquisition, and therefore 'live' imaging is not possible. For intermittent imaging during TSS, 'vertical field open' iMRI systems (Magnetom Open, Siemens AG, Erlangen, Germany, and Hitachi Airis II, Hitachi Medical Systems, Twinsburg, OH) were introduced.[10,31,33,35,37,43,44] These systems have a vertical C-arm construction, and allow greater lateral access to the patient, but, with restricted vertical access. Semi-portable horizontal field retractable iMRI[8,28–30,45–49] (PoleStar N-10 and PoleStar N-20, Odin Medical Technologies, Newton, MA) have gained popularity due to lower cost of implementation and due to the minimal operating room modifications required to implement the system. Higher field strength (≥ 1.5 T) iMRI systems[11,32,34,37,38,50–55] are exclusively in the conventional horizontal bore configuration. These iMRI systems are typically diagnostic quality machines adapted for use in the operating room, and can be routinely used for diagnostic imaging as a shared-resource.[33,34,55]

Room configuration—Room configurations for iMRIs have progressively evolved. Single use iMRI systems as originally installed required significant infrastructure modification and investment. Twin operating rooms with a shared iMRI improves the efficiency of iMRI machines by allowing multiple surgical procedures to take place with staggered intra-operative imaging. Similarly, a shared-resource strategy allowed diagnostic use of iMRI systems during operating room down-time. High field strength (≥ 1.5 T) iMRI machines are now typically implemented as a shared-resource with diagnostic radiology. At the NIH Clinical Center, we have implemented a single room, shared-resource iMRI configuration based on a 1.5 T (Achieva, Phillips Healthcare, Andover, MA) horizontal bore machine (Figure 1).[56]

Indications for iMRI during TSS

Stereotaxy and neuronavigation—Modern iMRI systems integrate neuronavigation.[28] During the initial approach to the sella, pre-operatively obtained images enable neuronavigation and stereotaxy. The advantage of iMRI systems is that they provide updated imaging during the initial approach, and periodically during the procedure. Images obtained with nasal speculum in place guide adjustment of the plane of approach to the sella (stereotaxy).[26] Subsequently, the surgeon can evaluate critical structures beyond visibility using updated intra-operative imaging (neuronavigation).[10], Neuronavigation using updated imaging during TSS is especially useful during redo TSS procedures[57] because scarring and adhesions distort the anatomy along the surgical corridor, with limited visualization of distal anatomy.

Resection control—For resection control, iMRI enabled visualization of unexpected tumor remnants[32,58,59], decompression of the optic chiasm[29,35,37], identification of the normal pituitary gland[43,60], and the changing configuration of tumor margins with debulking. Detection of unexpected remnants prompts targeted removal of residual tumor. This can lead to improved rates of GTR in non-functioning adenomas and other sellar tumors, as well as improved rates of biochemical remission in functioning adenomas.[9] Many large sellar tumors have significant extension to the cavernous sinuses or suprasellar regions and are not amenable for GTR. The real-world value of iMRI systems lie in detecting ‘actionable’ tumors detected as unexpected residuals. Intra-operative imaging is typically performed when the surgeon determines that a maximal possible resection has been achieved.[61] To determine the value of iMRI systems, we have to take into account the proportion of patients with unexpected residuals and the proportion of unexpected residuals that are ‘actionable’. Many authors reporting on utility of iMRI in TSS report a distinction between unexpected residuals and actionable unexpected residuals.[8,10,40,45,49,51,52,55] In general, intra-operative unexpected residuals are detected in up to 42% ± 18% (range 15% to 83%) of cases, of which re-exploration was attempted in 36% ± 17% (range 9% to 83%) (Table 1). Further tumor resection occurred in 33% ± 18% (range 9% to 83%) of the cases. No statistically significant differences in rates of detection of unexpected residuals or re-exploration were found between the studies utilizing low field (42%, 39%) high field (49%, 33%) and ultra-high field (27%, 26%) iMRI systems respectively (Figure 2). When aggregated, iMRI studies using endoscopes report a smaller proportion of unexpected residuals (34% ± 26%) than those using microscope (44% ± 18%) for TSS ($p = 0.04$, difference 10%, 95% CI 2.6% – 17.5%). Any such direct comparison of rates of residual tumor detection between studies reporting on endoscopic and microscopic approaches carries historical biases.[62] However, this is the best, albeit indirect, evidence available. Two large studies that comprised endoscopic and microscopic TSS cohorts, did not examine the differences in rates of unexpected tumor residuals between the two approaches.[41,63] Recent studies confirm the utility of iMRI in detecting actionable unexpected tumor residuals even in endoscopic TSS procedures.[58,64]

Detection and removal of unexpected residuals leads to increased extent of resection (EOR) for non-functioning tumors and improved endocrinological remission rates for hormone secreting adenomas. Many excellent reviews have examined the effect of iMRI on extent of

resection.[9,39] Following maximal resection prior to iMRI, intra-operative imaging can increase the likelihood of MRI-validated gross total resection (GTR) by 15 – 40%. Remarkably, in those patients that had been assigned for GTR, iMRI consistently increased the rate of GTR by 12% – 47%.[39] In patients with hormone secreting adenomas, intra-operative imaging can detect small residuals, whose targeted removal provides a 5% – 19% increase in rates of endocrinological remission.[11,46] In a large, single center study, iMRI prompted further tumor resection in 9% of cases. A statistically significant improvement in EOR occurred in cases with iMRI and endoscopy vs. non-iMRI, microscopic cases (OR 2.05, 95% CI 1.21 – 3.46, $p < 0.001$). However, implementation of either iMRI or endoscopy alone did not significantly affect biochemical remission rates ($p = 0.93$).[63]

Complication detection and avoidance—Updated imaging during the procedure can detect hematomas within the surgical field.[26,28,33,34,36,40] Since, acute hematoma may appear iso-intense to normal tissue on routine T1W imaging[10], centers now routinely include MRI sequences designed to detect developing blood clots such as turbo spin echo[10] or gradient recalled echo.[27,36] With high resolution T2W imaging possible with 3 T iMRI systems, developing hematomas may be distinguished from tumor remnants without the use of intravenous contrast.[9,34] Intra-operative imaging also demonstrates proximity to the optic apparatus and the carotid arteries, and successful decompression of the optic chiasm.[57] Intraoperative multiplanar imaging is especially useful for avoiding complications and improving EOR in giant (> 4 cm) pituitary adenomas. Three dimensional imaging of distorted anatomical structures and detection of residual tumor unobserved through the microscope or endoscope can improve during resection of these large adenomas.[47]

Microadenoma detection—Low field strength iMRI (0.2 T) systems often cannot resolve the presence of microadenomas during TSS[65], and currently, the utility of iMRI in TSS for microadenomas remains limited.[31] Although, low field strength iMRIs may not detect otherwise MRI-invisible microadenomas, intra-operative imaging may have a limited role in confirming GTR during TSS. Walker et al. reported that GTR of four microadenomas was confirmed by 0.5 T ‘double doughnut’ iMRI (1 growth hormone secreting, and 3 non-functioning).[40] For functioning microadenomas secreting growth hormone, no microadenomas (0/10) were detected with tumor remnant at follow-up, confirming the findings of iMRI findings in a low field (0.2 T) machine.[46] Using a high-field iMRI system (1.5 T) and volumetric imaging, small adenoma remnants may be detected leading to improved endocrine remission.[11] Similarly, ultra-high field systems can confirm radical resection of microadenomas prior to TSS completion[32], but, may not be useful in improving the detection of MRI invisible microadenomas or cavernous sinus invasion.

Safety/Pitfalls of using iMRI during TSS

Implementation of iMRI extends operating room time by approximately 2 hours.[63] Despite lengthening operating room time and duration of anesthesia, instances of complications attributable to iMRI are rare.[38] Overall, iMRI use for TSS remains safe, with no reported increase in complications from its implementation.[39,48,53] Faster image acquisition using higher field strength magnets reduces imaging duration. Despite this, surgeons may often choose to perform TSS without iMRI in patients with significant co-morbidities.[63]

Interpretation of intra-operative imaging is challenging[29,43], and instances of false-positive detections have been confirmed by histopathology and/or post-operative imaging. The instances of false-positive cases led to a recent evidence-based guideline from the Congress of Neurological Surgeons that recommended against iMRI for TSS.[66] High-resolution T2W imaging possible with ultra-high field strength machines will likely reduce the rates of false positive detection of tumor residual.[32]

Future directions

At the NIH Clinical Center, we have focused on improving imaging detection of microadenomas causing Cushing's disease.[67–70] In imaging terms, improved detection would result from improved spatial resolution and an increase in signal to noise ratio (SNR).[71,72] In iMRI systems, increasing magnetic field strength leads to a proportional increase in SNR. Increasing the field strength of existing iMRI systems is often financially unfeasible because such iMRI systems are more expensive and require significant infrastructure modification. Novel surface coils may be cost effective alternatives for increasing the SNR and/or resolution of images. They were first described to successfully detect chemical compounds in localized regions adjacent to the coils.[73] Currently, iMRI systems are coupled with custom designed surface coils during TSS.[10,27,50] However, surface coils are not ideal for imaging structures in the center of the body or head. In the center of the head, any increase in signal by using surface coils may be counteracted by a corresponding rise in correlated noise, leading to no net increase in SNR.[71] Location of the pituitary gland and the sella in the center of the cranium makes these sites poor targets for conventional surface coils used in preoperative and intraoperative imaging.

Following the principles used to design the endorectal coil[74], we have developed an endosphenoidal coil (ESC) to improve imaging of the sellar and parasellar structures during TSS (Figure 3).[69] We tested the ESC in cadavers using an existing iMRI system (1.5 T, Achieva, Phillips Healthcare) and demonstrated that SNR values 5 – 12 (mean 10.9 ± 1.6) times those achievable with conventional surface coils. We also showed that ultra-high resolution imaging of the sella (voxel size = 0.15 × 0.15 × 0.3 mm^3) could be achieved within a reasonable image acquisition time (~ 6 minutes). We hope to incorporate the ESC within the existing iMRI system to improve detection of otherwise MRI-invisibile microadenomas (Figure 4) in patients with Cushing's disease.

Conclusions

Intraoperative MRI during transsphenoidal surgery with microscope or endoscope leads to increased detection of actionable, unexpected tumor residuals which can improve the rate of gross total resection and/or biochemical remission. Implementation of iMRI systems during TSS is safe. High-field and ultra-high field iMRI systems are more expensive that lower field systems, but can reduce image acquisition time, improve the signal-to-noise ratio and improve the resolution of resulting images. Shared-resource strategy can be used to offset the costs of iMRI implementation.

Acknowledgments

The study was supported by the Intramural Research Program of the National Institute of Neurological Diseases and Stroke.

References

1. Swearingen B. Update on pituitary surgery. J Clin Endocrinol Metab. 2012; 97(4):1073–1081. DOI: 10.1210/jc.2011-3237 [PubMed: 22337908]
2. Biller BMK, Grossman aB, Stewart PM, et al. Treatment of adrenocorticotropin-dependent Cushing's syndrome: a consensus statement. J Clin Endocrinol Metab. 2008; 93(7):2454–2462. DOI: 10.1210/jc.2007-2734 [PubMed: 18413427]
3. Giustina, a, Chanson, P., Bronstein, MD., et al. A consensus on criteria for cure of acromegaly. J Clin Endocrinol Metab. 2010; 95(7):3141–3148. DOI: 10.1210/jc.2009-2670 [PubMed: 20410227]
4. Liu JK, Das K, Weiss MH, Laws ER, Couldwell WT. The history and evolution of transsphenoidal surgery. J Neurosurg. 2001; 95(6):1083–1096. DOI: 10.3171/jns.2001.95.6.1083 [PubMed: 11765830]
5. Henderson WR. The pituitary adenomata. A follow-up study of the surgical results in 338 cases. (DR. HARVEY CUSHING'S SERIES). Br J Surg. 1939; 26(104):811–921. DOI: 10.1002/bjs.18002610417
6. Roelfsema F, Biermasz NR, Pereira AM. Clinical factors involved in the recurrence of pituitary adenomas after surgical remission: a structured review and meta-analysis. Pituitary. 2012; 15(1):71–83. DOI: 10.1007/s11102-011-0347-7 [PubMed: 21918830]
7. Elias WJ, Chadduck JB, Alden TD, Laws ER. Frameless stereotaxy for transsphenoidal surgery. Neurosurgery. 1999; 45(2):271-5-7. [PubMed: 10449071]
8. Berkmann S, Fandino J, Zosso S, Killer HE, Remonda L, Landolt H. Intraoperative magnetic resonance imaging and early prognosis for vision after transsphenoidal surgery for sellar lesions. J Neurosurg. 2011; 115(3):518–527. DOI: 10.3171/2011.4.JNS101568 [PubMed: 21639700]
9. Buchfelder M, Schlaffer S-M. Intraoperative magnetic resonance imaging during surgery for pituitary adenomas: pros and cons. Endocrine. 2012; 42(3):483–495. DOI: 10.1007/s12020-012-9752-6 [PubMed: 22833429]
10. Steinmeier R, Fahlbusch R, Ganslandt O, et al. Intraoperative magnetic resonance imaging with the magnetom open scanner: concepts, neurosurgical indications, and procedures: a preliminary report. Neurosurgery. 1998; 43(4):739-47-8. [PubMed: 9766299]
11. Tanei T, Nagatani T, Nakahara N, et al. Use of high-field intraoperative magnetic resonance imaging during endoscopic transsphenoidal surgery for functioning pituitary microadenomas and small adenomas located in the intrasellar region. Neurol Med Chir (Tokyo). 2013; 53(7):501–510. [PubMed: 23883562]
12. Hardy J, Wigser SM. Trans-sphenoidal surgery of pituitary fossa tumors with televised radiofluoroscopic control. J Neurosurg. 1965; 23(6):612–619. DOI: 10.3171/jns.1965.23.6.0612 [PubMed: 5861144]
13. Asthagiri AR, Laws ER, Jane JA. Image guidance in pituitary surgery. Front Horm Res. 2006; 34:46–63. DOI: 10.1159/000091571 [PubMed: 16474215]
14. Jane JA, Thapar K, Alden TD, Laws ER. Fluoroscopic frameless stereotaxy for transsphenoidal surgery. Neurosurgery. 2001; 48(6):1302-7-8. [PubMed: 11383734]
15. Suzuki R, Asai J, Nagashima G, et al. Transcranial echo-guided transsphenoidal surgical approach for the removal of large macroadenomas. J Neurosurg. 2004; 100(1):68–72. DOI: 10.3171/jns.2004.100.1.0068 [PubMed: 14743914]
16. Atkinson JLD, Kasperbauer JL, James EM, Lane JI, Nippoldt TB. Transcranial-transdural real-time ultrasonography during transsphenoidal resection of a large pituitary tumor. J Neurosurg. 2000; 93:129–131. DOI: 10.3171/jns.2000.93.1.0129 [PubMed: 10883916]
17. Arita K, Kurisu K, Tominaga a, et al. Trans-sellar color Doppler ultrasonography during transsphenoidal surgery. Neurosurgery. 1998; 42(1):81–5. discussion 86. [PubMed: 9442507]

18. Solheim O, Selbekk T, Løvstakken L, et al. Intrasellar ultrasound in transsphenoidal surgery: a novel technique. Neurosurgery. 2010; 66(1):173-85-6.doi: 10.1227/01.NEU.0000360571.11582.4F
19. Ota Y, Mami I. Ultrasonography imaging during nasal endoscopic transsphenoidal surgery. ORL J Otorhinolaryngol Relat Spec. 2013; 75(1):27–31. DOI: 10.1159/000346931 [PubMed: 23548466]
20. Doppman JL, Ram Z, Shawker TH, Oldfield EH. Intraoperative US of the pituitary gland. Work in progress. Radiology. 1994; 192(1):111–115. DOI: 10.1148/radiology.192.1.8208921 [PubMed: 8208921]
21. Watson JC, Shawker TH, Nieman LK, Devroom HL, Doppman JL, Oldfield EH. Localization of pituitary adenomas by using intraoperative ultrasoound pituitary in patients with Cushing's disease and no demonstrable tumor on magnetic resonance imaging. J Neurosurg. 1998; 89(6):927–932. [PubMed: 9833817]
22. Lufkin R, Teresi L, Hanafee W. New needle for MR-guided aspiration cytology of the head and neck. AJR Am J Roentgenol. 1987; 149(2):380–382. DOI: 10.2214/ajr.149.2.380 [PubMed: 3496765]
23. Grönemeyermd DHW, Seibelmd RMM, Melzermd a, et al. Future of advanced guidance techniques by interventional CT and MRI. Minim Invasive Ther Allied Technol. 1995; 4(5–6): 251–259. DOI: 10.3109/13645709509152803
24. Jolesz FA, Blumenfeld SM. Interventional use of magnetic resonance imaging. Magn Reson Q. 1994; 10(2):85–96. [PubMed: 7986703]
25. Black PM, Moriarty T, Alexander E, et al. Development and implementation of intraoperative magnetic resonance imaging and its neurosurgical applications. Neurosurgery. 1997; 41(4): 831-42-5. [PubMed: 9316044]
26. Martin CH, Schwartz R, Jolesz F, Black PM. Transsphenoidal resection of pituitary adenomas in an intraoperative MRI unit. Pituitary. 1999; 2(2):155–162. [PubMed: 11081166]
27. Schwartz RB, Hsu L, Wong TZ, et al. Intraoperative MR imaging guidance for intracranial neurosurgery: experience with the first 200 cases. Radiology. 1999; 211(2):477–488. DOI: 10.1148/radiology.211.2.r99ma26477 [PubMed: 10228532]
28. Kanner AA, Vogelbaum MA, Mayberg MR, Weisenberger JP, Barnett GH. Intracranial navigation by using low-field intraoperative magnetic resonance imaging: preliminary experience. J Neurosurg. 2002; 97(5):1115–1124. DOI: 10.3171/jns.2002.97.5.1115 [PubMed: 12450034]
29. Schwartz TH, Stieg PE, Anand VK. Endoscopic transsphenoidal pituitary surgery with intraoperative magnetic resonance imaging. Neurosurgery. 2006; 58(SUPPL 1):44–51. DOI: 10.1227/01.NEU.0000193927.49862.B6
30. Gerlach R, Du Mesnil De Rochemont R, Gasser T, et al. Feasibility of polestar N20, an ultra-low-field intraoperative magnetic resonance imaging system in resection control of pituitary macroadenomas: Lessons learned from the first 40 cases. Neurosurgery. 2008; 63(2):272–284. DOI: 10.1227/01.NEU.0000312362.63693.78 [PubMed: 18797357]
31. Bohinski RJ, Warnick RE, Gaskill-Shipley MF, et al. Intraoperative magnetic resonance imaging to determine the extent of resection of pituitary macroadenomas during transsphenoidal microsurgery. Neurosurgery. 2001; 49(5):1133–1144. DOI: 10.1227/00006123-200111000-00023 [PubMed: 11846908]
32. Netuka D, Masopust V, Belšán T, Kramáø F, Beneš V. One year experience with 3.0 T intraoperative MRI in pituitary surgery. Acta Neurochir Suppl. 2011; 109(10):157–159. DOI: 10.1007/978-3-211-99651-5_24 [PubMed: 20960336]
33. McPherson CM, Bohinski RJ, Dagnew E, Warnick RE, Tew JM. Tumor resection in a shared-resource magnetic resonance operating room: experience at the University of Cincinnati. Acta Neurochir Suppl. 2003; 85:39–44. [PubMed: 12570136]
34. Pamir MN. 3 T ioMRI: the Istanbul experience. Acta Neurochir Suppl. 2011; 109(10):131–137. DOI: 10.1007/978-3-211-99651-5_20 [PubMed: 20960332]
35. Hlavin ML, Lewin JS, Arafah BM, Cesar A, Clampitt M, Selman WR. Intraoperative magnetic resonance imaging for assessment of chiasmatic decompression and tumor resection during transsphenoidal pituitary surgery. Tech Neurosurg. 2000; 6(4)

36. Pergolizzi RS, Nabavi A, Schwartz RB, et al. Intra-operative MR guidance during trans-sphenoidal pituitary resection: Preliminary results. J Magn Reson Imaging. 2001; 13(1):136–141. DOI: 10.1002/1522-2586(200101)13:1<136::AID-JMRI1021>3.0.CO;2-8 [PubMed: 11169816]
37. Nimsky C, Ganslandt O, Fahlbusch R. Comparing 0.2 Tesla with 1.5 Tesla intraoperative magnetic resonance imaging: Analysis of setup, workflow, and efficiency. Acad Radiol. 2005; 12(9):1065–1079. DOI: 10.1016/j.acra.2005.05.020 [PubMed: 16099691]
38. Nimsky C, Von Keller B, Ganslandt O, Fahlbusch R. Intraoperative high-field magnetic resonance imaging in transsphenoidal surgery of hormonally inactive pituitary macroadenomas. Neurosurgery. 2006; 59(1):105–113. DOI: 10.1227/01.NEU.0000219198.38423.1E
39. Patel KS, Yao Y, Wang R, Carter BS, Chen CC. Intraoperative magnetic resonance imaging assessment of non-functioning pituitary adenomas during transsphenoidal surgery. Pituitary. 2016; 19(2):222–231. DOI: 10.1007/s11102-015-0679-9 [PubMed: 26323592]
40. Walker DG, Black PML. Use of intraoperative MRI in pituitary surgery. Oper Tech Neurosurg. 2002; 5(4):231–238. DOI: 10.1053/otns.2002.32496
41. Vitaz TW, Inkabi KE, Carrubba CJ. Intraoperative MRI for transphenoidal procedures: Short-term outcome for 100 consecutive cases. Clin Neurol Neurosurg. 2011; 113(9):731–735. DOI: 10.1016/j.clineuro.2011.07.025 [PubMed: 21889838]
42. Kajiwara K, Nishizaki T, Ohmoto Y, Nomura S, Suzuki M. Image-Guided Transsphenoidal Surgery for Pituitary Lesions Using Mehrkoordinaten Manipulator (MKM) Navigation System. min - Minim Invasive Neurosurg. 2003; 46(2):78–81. DOI: 10.1055/s-2003-39340 [PubMed: 12761676]
43. Fahlbusch R, Ganslandt O, Buchfelder M, Schott W, Nimsky C. Intraoperative magnetic resonance imaging during transsphenoidal surgery. J Neurosurg. 2001; 95(3):381–390. DOI: 10.3171/jns.2001.95.3.0381 [PubMed: 11565857]
44. Nimsky C, Ganslandt O, Hofmann B, Fahlbusch R. Limited Benefit of Intraoperative Low-field Magnetic Resonance Imaging in Craniopharyngioma Surgery. Neurosurgery. 2003; 53(1):72–81. DOI: 10.1227/01.NEU.0000068728.08237.AF [PubMed: 12823875]
45. Wu JS, Shou XF, Yao CJ, et al. Transsphenoidal pituitary macroadenomas resection guided by PoleStar N20 low-field intraoperative magnetic resonance imaging: Comparison with early postoperative high-field magnetic resonance imaging. Neurosurgery. 2009; 65(1):63–70. DOI: 10.1227/01.NEU.0000348549.26832.51 [PubMed: 19574826]
46. Bellut D, Hlavica M, Schmid C, Bernays RL. Intraoperative magnetic resonance imaging-assisted transsphenoidal pituitary surgery in patients with acromegaly. Neurosurg Focus. 2010; 29(4):E9.doi: 10.3171/2010.7.FOCUS10164
47. Baumann F, Schmid C, Bernays RL. Intraoperative magnetic resonance imaging-guided transsphenoidal surgery for giant pituitary adenomas. Neurosurg Rev. 2010; 33(1):83–90. DOI: 10.1007/s10143-009-0230-4 [PubMed: 19823884]
48. Berkmann S, Fandino J, Müller B, Remonda L, Landolt H. Intraoperative MRI and endocrinological outcome of transsphenoidal surgery for non-functioning pituitary adenoma. Acta Neurochir (Wien). 2012; 154(4):639–647. DOI: 10.1007/s00701-012-1285-5 [PubMed: 22286656]
49. Hlavica M, Bellut D, Lemm D, Schmid C, Bernays RL. Impact of ultra-low-field intraoperative magnetic resonance imaging on extent of resection and frequency of tumor recurrence in 104 surgically treated nonfunctioning pituitary adenomas. World Neurosurg. 2013; 79(1):99–109. DOI: 10.1016/j.wneu.2012.05.032 [PubMed: 23043996]
50. Dort JC, Sutherland GR. Intraoperative magnetic resonance imaging for skull base surgery. Laryngoscope. 2001; 111(9):1570–1575. DOI: 10.1097/00005537-200109000-00014 [PubMed: 11568606]
51. Fahlbusch R, Keller BV, Ganslandt O, Kreutzer J, Nimsky C. Transsphenoidal surgery in acromegaly investigated by intraoperative high-field magnetic resonance imaging. Eur J Endocrinol. 2005; 153(2):239–248. DOI: 10.1530/eje.1.01970 [PubMed: 16061830]
52. Kuge A, Kikuchi Z, Sato S, Sakurada K, Takemura S, Kayama T. Practical use of a simple technique, insertion of wet cotton pledgets into the tumor resection cavity in transsphenoidal surgery of pituitary tumors, for a better comparison between pre- and intraoperative high-field

magnetic resonance images. J Neurol Surgery, Part A Cent Eur Neurosurg. 2013; 74(6):366–372. DOI: 10.1055/s-0033-1349342

53. Coburger J, König R, Seitz K, Bäzner U, Wirtz CR, Hlavac M. Determining the utility of intraoperative magnetic resonance imaging for transsphenoidal surgery: a retrospective study. J Neurosurg. Dec.2013 :1–11. DOI: 10.3171/2013.9.JNS122207
54. Berkmann S, Schlaffer S, Nimsky C, Fahlbusch R, Buchfelder M. Follow-up and long-term outcome of nonfunctioning pituitary adenoma operated by transsphenoidal surgery with intraoperative high-field magnetic resonance imaging. Acta Neurochir (Wien). 2014; 156(12): 2233–2243. DOI: 10.1007/s00701-014-2210-x [PubMed: 25174805]
55. Fomekong E, Duprez T, Docquier M-A, Ntsambi G, Maiter D, Raftopoulos C. Intraoperative 3T MRI for pituitary macroadenoma resection: Initial experience in 73 consecutive patients. Clin Neurol Neurosurg. 2014; 126:143–149. DOI: 10.1016/j.clineuro.2014.09.001 [PubMed: 25255158]
56. Weingarten DM, Asthagiri AR, Butman Ja, et al. Cortical mapping and frameless stereotactic navigation in the high-field intraoperative magnetic resonance imaging suite. J Neurosurg. 2009; 111(6):1185–1190. DOI: 10.3171/2009.5.JNS09164 [PubMed: 19499978]
57. Ahn JY, Jung JY, Kim J, Lee KS, Kim SH. How to overcome the limitations to determine the resection margin of pituitary tumours with low-field intra-operative MRI during trans-sphenoidal surgery: Usefulness of Gadolinium-soaked cotton pledgets. Acta Neurochir (Wien). 2008; 150(8): 763–771. DOI: 10.1007/s00701-008-1505-1 [PubMed: 18594752]
58. Zaidi HA, De Los Reyes K, Barkhoudarian G, et al. The utility of high-resolution intraoperative MRI in endoscopic transsphenoidal surgery for pituitary macroadenomas: early experience in the Advanced Multimodality Image Guided Operating suite. Neurosurg Focus. 2016; 40(3):E18.doi: 10.3171/2016.1.FOCUS15515 [PubMed: 26926058]
59. Theodosopoulos PV, Leach J, Kerr RG, et al. Maximizing the extent of tumor resection during transsphenoidal surgery for pituitary macroadenomas: can endoscopy replace intraoperative magnetic resonance imaging? J Neurosurg. 2010; 112(4):736–743. DOI: 10.3171/2009.6.JNS08916 [PubMed: 19835472]
60. Szerlip NJ, Zhang YC, Placantonakis DG, et al. Transsphenoidal resection of sellar tumors using high-field intraoperative magnetic resonance imaging. Skull Base. 2011; 21(4):223–232. DOI: 10.1055/s-0031-1277262 [PubMed: 22470265]
61. Schwartz TH. Editorial: Intraoperative magnetic resonance imaging and pituitary surgery. J Neurosurg. Dec.2013 :1–4. DOI: 10.3171/2013.7.JNS13956
62. Jane JA, Laws ER. Endoscopy versus MR imaging. J Neurosurg. 2010; 112(4):734. discussion 735. doi: 10.3171/2009.7.JNS091042 [PubMed: 19835473]
63. Sylvester PT, Evans Ja, Zipfel GJ, et al. Combined high-field intraoperative magnetic resonance imaging and endoscopy increase extent of resection and progression-free survival for pituitary adenomas. Pituitary. Mar.2014 doi: 10.1007/s11102-014-0560-2
64. Serra C, Burkhardt J-K, Esposito G, et al. Pituitary surgery and volumetric assessment of extent of resection: a paradigm shift in the use of intraoperative magnetic resonance imaging. Neurosurg Focus. 2016; 40(3):E17.doi: 10.3171/2015.12.FOCUS15564 [PubMed: 26926057]
65. Schulder M. Intracranial surgery with a compact, low-field-strength magnetic resonance imager. Top Magn Reson Imaging. 2009; 19(4):179–189. DOI: 10.1097/RMR.0b013e31819637cc [PubMed: 19148034]
66. Aghi MK, Chen CC, Fleseriu M, et al. Congress of Neurological Surgeons Systematic Review and Evidence-Based Guidelines on the Management of Patients with Nonfunctioning Pituitary Adenomas: Executive Summary. Neurosurgery. 2016; 79(4):521–523. DOI: 10.1227/NEU. 0000000000001386 [PubMed: 27635956]
67. Patronas N, Bulakbasi N, Stratakis CA, et al. Spoiled gradient recalled acquisition in the steady state technique is superior to conventional postcontrast spin echo technique for magnetic resonance imaging detection of adrenocorticotropin-secreting pituitary tumors. J Clin Endocrinol Metab. 2003; 88(4):1565–1569. DOI: 10.1210/jc.2002-021438 [PubMed: 12679440]
68. Chittiboina P, Montgomery BK, Millo C, Herscovitch P, Lonser RR. High-resolution 18 F-fluorodeoxyglucose positron emission tomography and magnetic resonance imaging for pituitary

adenoma detection in Cushing disease. J Neurosurg. 2014; 122(April):1–7. DOI: 10.3171/2014.10.JNS14911

69. Chittiboina P, Lalith Talagala S, Merkle H, et al. Endosphenoidal coil for intraoperative magnetic resonance imaging of the pituitary gland during transsphenoidal surgery. J Neurosurg. Mar.2016 : 1–9. DOI: 10.3171/2015.11.JNS151465
70. Mehta GU, Montgomery BK, Raghavan P, et al. Different imaging characteristics of concurrent pituitary adenomas in a patient with Cushing's disease. J Clin Neurosci. 2015; 22(5):891–894. DOI: 10.1016/j.jocn.2015.01.001 [PubMed: 25827866]
71. Redpath TW. Signal-to-noise ratio in MRI. Br J Radiol. 1998; 71(847):704–707. [PubMed: 9771379]
72. Magee T, Shapiro M, Williams D. Comparison of high-field-strength versus low-field-strength MRI of the shoulder. AJR Am J Roentgenol. 2003; 181(5):1211–1215. DOI: 10.2214/ajr.181.5.1811211 [PubMed: 14573405]
73. Ackerman JJ, Grove TH, Wong GG, Gadian DG, Radda GK. Mapping of metabolites in whole animals by 31P NMR using surface coils. Nature. 1980; 283(5743):167–170. [PubMed: 7350541]
74. Schnall MD, Imai Y, Tomaszewski J, Pollack HM, Lenkinski RE, Kressel HY. Prostate cancer: local staging with endorectal surface coil MR imaging. Radiology. 1991; 178(3):797–802. DOI: 10.1148/radiology.178.3.1994421 [PubMed: 1994421]
75. Jiménez P, Brell M, Sarriá-Echegaray P, Roldán P, Tomás-Barberán M, Ibáñez J. "Intrasellar Balloon Technique" in intraoperative MRI guided transsphenoidal endoscopic surgery for sellar region tumors. Usefulness on image interpretation and extent of resection evaluation. Technical note. Acta Neurochir (Wien). 2016; doi: 10.1007/s00701-015-2697-9

Key Points

1. Low and high field iMRI is used for resection control of pituitary macroadenomas
2. Expert interpretation of iMRI images is required to achieve best results
3. iMRI can improve outcomes of non-functioning and functioning pituitary macroadenomas
4. iMRI is not useful to detect functioning pituitary microadenomas

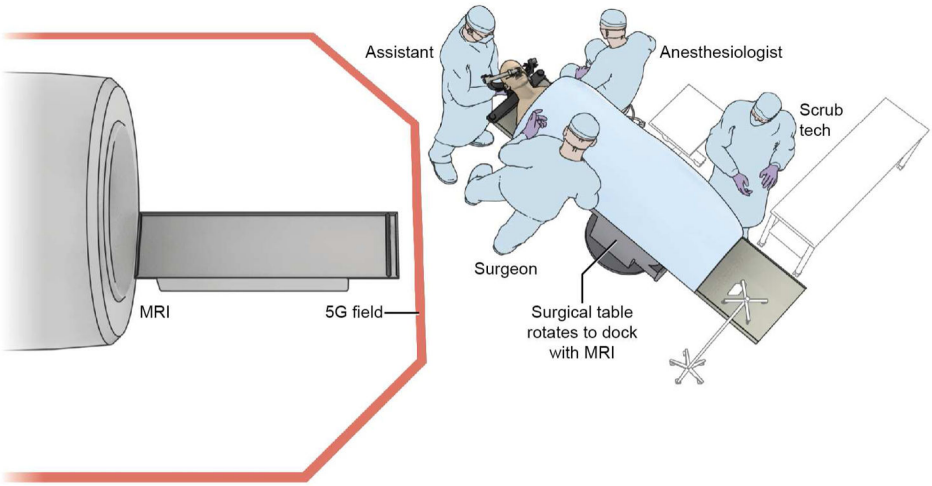

Figure 1.

The high field (1.5 Tesla) iMRI system at the Clinical Center of National Institutes of Health, Bethesda, MD. The initial surgical approach is performed on the surgical table as usual. An MR imaging–compatible patient reference frame (Polestar, Medtronic, Inc.) is attached to the head holder using an MR imaging–compatible, custom-designed patient reference frame holder (Integra Life Sciences Corp.). The neuronavigation system (StealthStation, Medtronic Inc.) is registered and a microscopic or endoscopic transsphenoidal approach, and initial adenoma resection is performed. For intra-operative imaging, the surgical table is rotated to dock with the iMRI. Following image acquisition, the subject is brought back outside the 5 Gauss (5G) field line for resumption of the surgical process and/or closure.

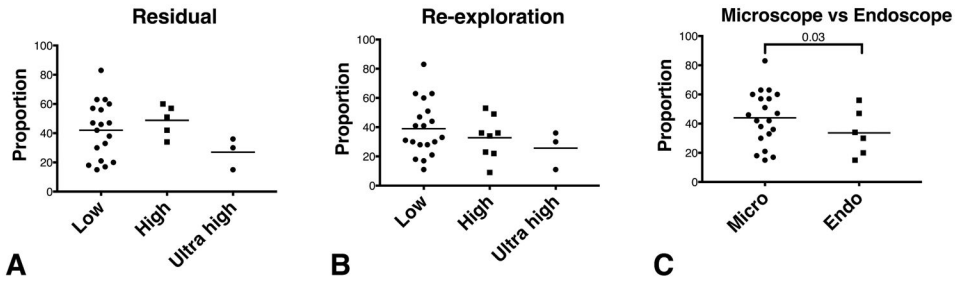

Figure 2.

Unexpected tumor residuals reported in the studies included in this review. Studies that explicitly reported unexpected tumor residuals following maximal initial resection (Table 1) are analyzed here. The reported proportions of cases with unexpected residuals was not statistically significantly different with the strength of the magnetic field in iMRI studies (A). Similarly, no differences were found in the proportion of cases that underwent a re-exploration following intra-operative imaging (B). A statistically significant lower occurrence of unexpected residuals ($p = 0.03$) was reported in studies reporting an endoscopic approach compared to ones reporting a microscopic approach (C). High – high field strength magnet, 1.5 Tesla; Low – low field strength magnet, ≥ 0.5 Tesla; Ultra high ≥ 3Tesla field strength magnets.

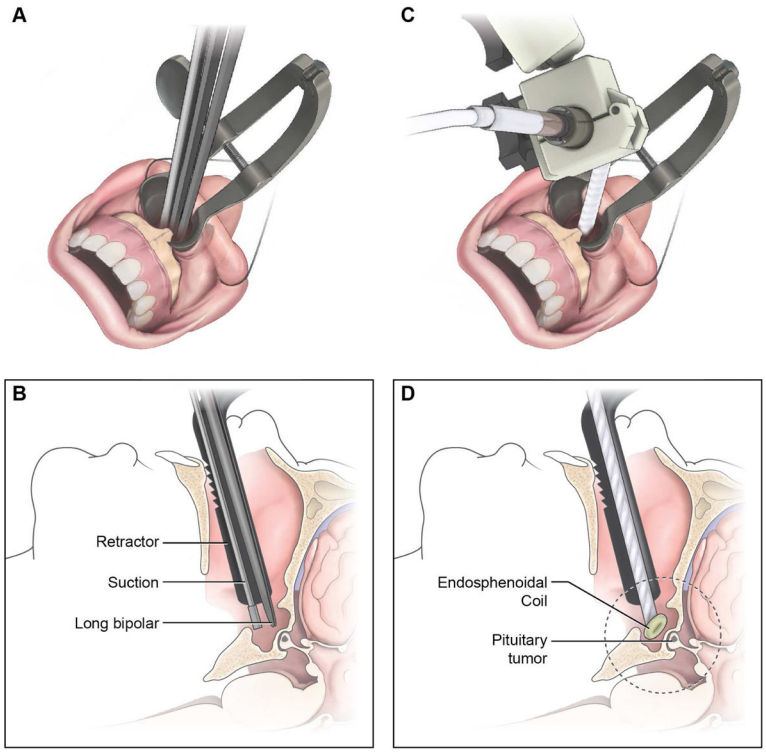

Figure 3.

Positioning of the ensdosphenoidal coil (ESC) within the surgical path created during TSS. Standard approach to the sella involves creating a surgical tract, removal of sphenoid wall and insertion of MRI self-retaining retractors (A). The surgical corridor allows for insertion of instruments such as suction and bipolar cautery devices (B). Following initial approach, the ESC can be placed within the surgical corridor (C) such that the distal coil reaches within the sphenoid sinus (D).

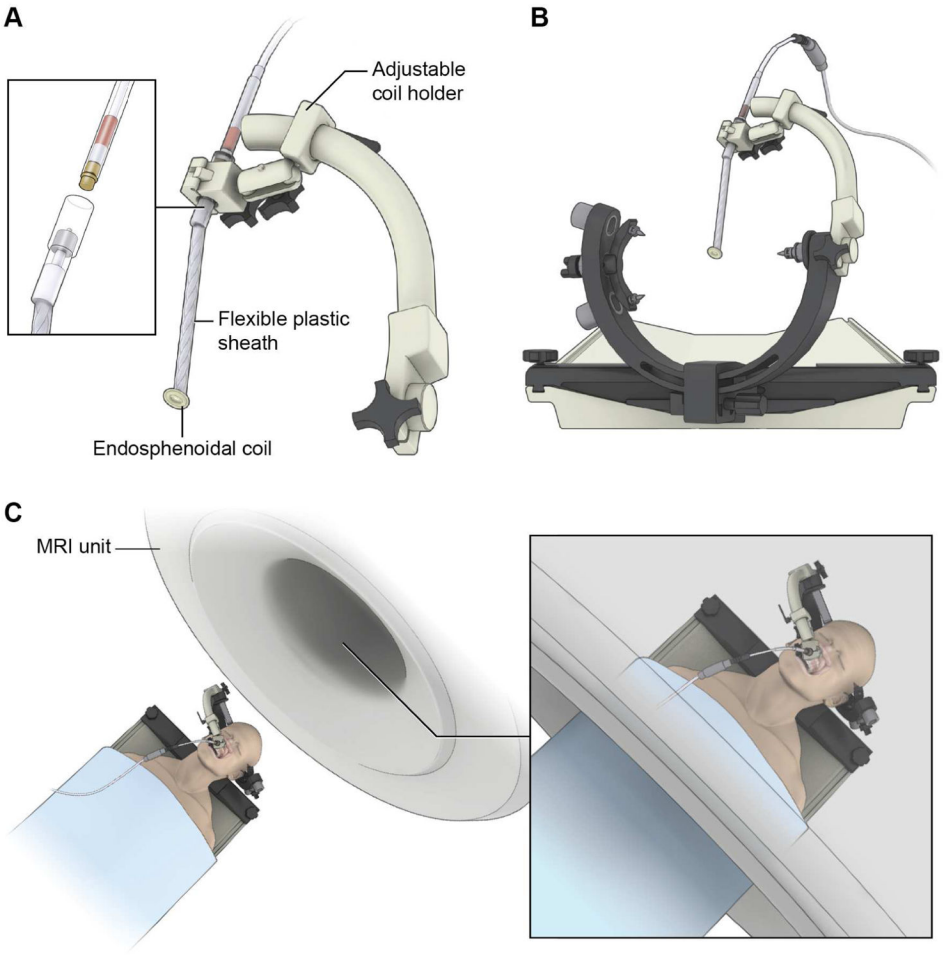

Figure 4.

Once the endosphenoidal coil (ESC) is in place within the surgical corridor, it is secured to the head holder with a custom coil holder (A). The ESC is attached to the interface box (inset). The custom coil holder attaches to the standard three-point cranial fixation device (B). When fixed, the subject will be moved into the MRI bore (inset) for image acquisition (C).

Table 1

List of the iMRI studies reported in this manuscript.

Ref	Study	TSS type	Manufacturer and Room Design	Magnet Field Strength and Field type	Number of tumors/ NFPA/ Macroadenoma/ Microadenoma	Unexpected residual (%)	Cases re-explored (%)	Further resection possible (%)
			Low Field iMRI					
10	1998, Steinmeier, Erlangen	Microscope	Siemens Magnetom Open, Twin room, moving table/Single room, moving table	0.2 T, Vertical field open	18/ 15/ 18/ 0	6 (33)	5 (28)	3 (17)
26	1999, Martin, Boston	Microscope	GE Signa SP, Single room	0.5 T, Double Doughnut	5/ 2/ 5/ 0	3 (60)	3 (60)	3 (60)
27	1999, Schwartz, Boston	Microscope	GE Signa SP, Single room	0.5 T, Double Doughnut	5/ -/ -/ -	- (-)	- (-)	- (-)
35	2000, Hlavin, Cleveland	Microscope	Siemens Magnetom Open, Single room, moveable table	0.2 T, Vertical field open	1/ 1/ 1/ 0	- (-)	- (-)	- (-)
31	2001, Bohinsky, Cincinnati	Microscope	Hitachi AIRIS II, Twin room, moving table/Single room, moving table	0.3 T, Vertical field open	30/ 22/ 30/ 0	19 (63)	19 (63)	19 (63)
43	2001, Fahlbusch, Erlangen	Microscope	Siemens Magnetom Open, Twin room, moving table/Single room, moving table	0.2 T, Vertical field open	44/ 39/ 44/ 0	- (-)	- (-)	- (-)
36	2001, Pergolizzi, Boston	Microscope	GE Signa SP, Single room	0.5 T, Double Doughnut	17/ -/ -/ -	- (-)	- (-)	- (-)
40	2002, Walker, Boston	Microscope	GE Signa SP, Single room	0.5 T, Double Doughnut	23/ -/ 19/ 4	13 (57)	7 (30)	7 (30)
28	2002, Kanner, Cleveland	Microscope	Odin PoleStar N-10, Retractable magnet	0.12 T, Horizontal field open	9/ 8/ 0/ -	- (-)	- (-)	- (-)
44	2003, Nimsky, Erlangen	Microscope	Siemens Magnetom Open, Twin room, moving table/Single room, moving table	0.2 T, Vertical field open	6/ 0/ 6/ 0	1 (17)	1 (17)	1 (17)
33	2003, McPherson, Cincinnati	Microscope	Hitachi AIRIS II, Twin room, moving table/Single room, moving table	0.3 T, Vertical field open	30/ 22/ 30/ 0	19 (63)	19 (63)	19 (63)
37	2005, Nimsky, Erlangen*	Microscope	Siemens Magnetom Open, Twin room, moving table/Single room, moving table	0.2 T, Vertical field open	59/ -/ 59/ 0	- (-)	30 (51)	17 (29)
29	2006, Anand, New York	Endoscope	Odin PoleStar N-10, Retractable magnet	0.12 T, Horizontal field open	10/ 2/ 10/ 0	2 (20)	- (-)	- (-)
29	2006, Schwartz, New York	Endoscope	Odin PoleStar N-10, Retractable magnet	0.12 T, Horizontal field open	15/ 12/ 15/ 0	7 (47)	7 (47)	3 (20)

Ref	Study	TSS type	Manufacturer and Room Design	Magnet Field Strength and Field type	Number of tumors/ NFPA/ Macroadenoma/ Microadenoma	Unexpected residual (%)	Cases re-explored (%)	Further resection possible (%)
57	2007, Ahn, Seoul	Microscope	Odin Polestar N-20, Retractable magnet	0.15 T, Horizontal field open	63/ -/ -/ 0	19 (30)	19 (30)	19 (30)
30	2008, Gerlach, Frankfurt am Main	Microscope	Odin Polestar N-20, Retractable magnet	0.15 T, Horizontal field open	40/ 28/ 40/ 0	7 (18)	7 (18)	- (-)
45	2009, Wu, Shanghai	Microscope	Odin Polestar N-20, Retractable magnet	0.15 T, Horizontal field open	55/ -/ 55/ 0	23 (42)	17 (31)	9 (16)
46	2010, Bellut, Zurich	Microscope	Odin Polestar N-20, Retractable magnet	0.15 T, Horizontal field open	39/ 0/ 49/ 10	8 (21)	8 (21)	8 (21)
47	2010, Baumann, Zurich	Microscope	Odin Polestar N-20, Retractable magnet	0.15 T, Horizontal field open	6/ 5/ 6/ 0	5 (83)	5 (83)	5 (83)
59	2010, Theodosopoulos, Cincinnati	Endoscope	Hitachi AIRIS II, Twin room, moving table/Single room, moving table	0.3 T, Horizontal bore	27/ 10/ 27/ 0	4 (15)	3 (11)	3 (11)
41	2011, Vitaz, Louiseville	Both	GE Signa SP, Double Donut	0.5 T, Double Doughnut	100/ -/ 81/ 9	- (-)	41 (41)	41 (41)
8	2011, Berkmann, Aarau	Microscope	Odin Polestar N-20, Retractable magnet	0.15 T, Horizontal field open	32/ 26/ 32/ 0	15 (47)	9 (28)	9 (28)
48	2012, Berkmann, Aarau	Microscope	Odin Polestar N-20, Retractable magnet	0.15 T, Horizontal field open	60/ 60/ 60/ 0	23 (38)	20 (33)	20 (33)
49	2013, Hlavica, Zurich	Microscope	Odin Polestar N-20, Retractable	0.15 T, Horizontal field open	104/ 104/ -/ -	48 (46)	43 (41)	43 (41)
75	2016, Jimenez, Palma de Mallorca	Endoscope	Odin Polestar N-20, Single room	0.15 T, Horizontal field open	18/ 10/ -/ -	10 (56)	8 (44)	8 (44)
			High Field iMRI					
50	2001, Dort, Calgary	Microscope	Marconi IMRIS, Single room, moveable magnet	1.5 T, Horizontal bore	15/ -/ -/ -	9 (60)	8 (53)	8 (53)
37	2005, Nimsky, Erlangen	Microscope	Siemens Magneton Sonata, Single room, moveable table	1.5 T, Horizontal bore	129/ -/ 129/ 0	- (-)	30 (23)	28 (22)
51	2005, Fahlbusch, Erlangen	Microscope	Siemens Magneton Sonata, Single room, moveable table	1.5 T, Horizontal bore	23/ 0/ 23/ 0	13 (57)	5 (22)	5 (22)

Ref	Study	TSS type	Manufacturer and Room Design	Magnet Field Strength and Field type	Number of tumors/ NFPA/ Macroadenoma/ Microadenoma	Unexpected residual (%)	Cases re-explored (%)	Further resection possible (%)
38	2006, Nimsky, Erlangen*	Microscope	Siemens Magneton Sonata, Single room	1.5 T, Horizontal bore	85/ 85/ 85/ 0	36 (42)	29 (34)	29 (34)
60	2011, Szerlip, New York	Microscope	Siemens Espree, Single room	1.5 T, Horizontal bore	59/ -/ -/ -	30 (51)	29 (49)	- (-)
11	2013, Tanei, Nagoya	Endoscope	Siemens Magnetom Symphony,	1.5 T, Horizontal bore	14/ 0/ 7/ 7	7 (50)	5 (36)	5 (36)
52	2013, Kuge, Yamagata	Endoscope	GE Signa HDx, Twin operating room	1.5 T, Horizontal bore	35/ 27/ -/ -	12 (34)	3 (9)	3 (9)
53	2013, Coburger, Gunzburg	Microscope	Siemens Espree, Single room	1.5 T, Horizontal bore	76/ 52/ -/ -	- (-)	- (-)	- (-)
54	2014, Berkmann, Erlangen	Microscope	Siemens Magneton Sonata,	1.5 T, Horizontal bore	85/ -/ -/ -	- (-)	- (-)	- (-)
63	2014, Sylvester, St. Louis	Both	Siemens Espree, Twin operating room, moveable magnet	1.5 T, Horizontal bore	156/ 90/ -/ -	- (-)	56 (36)	56 (36)
58	2016, Zaidi, Boston	Endoscope	Siemens Verio, Single room, moveable magnet	3 T, Horizontal bore	20/ 11/ -/ -	6 (30)	6 (30)	6 (30)
			Ultra-high Field iMRI					
32	2011, Netuka, Prague	Microscope	GE Signa HDx, Twin operating room	3 T, Horizontal bore	85/ -/ 75/ 10	31 (36)	31 (36)	- (-)
34	2011, Pamir, Istanbul	Microscope	Siemens Trio, Twin operating room, Shared resource	3 T, Horizontal bore	42/ 42/ -/ -	- (-)	- (-)	- (-)
55	2014, Fomekong, Brussels	Microscope	Phillips Intera, Twin operating room	3 T, Horizontal bore	73/ -/ -/ -	11 (15)	8 (11)	8 (11)
64	2016, Serra, Zurich	Endoscope	Siemens Skyra, Twin operating room	3 T, Horizontal bore	50/ 33/ -/ -	- (-)	- (-)	- (-)
	Totals				**1763/ 706/ 906/ 40**	**(42)**	**(36)**	**(33)**

Relevant information including the date of publication, the first author and the city where the study was reported from are listed. Where available, data on the total number of tumors studied, the number of non-functioning pituitary adenomas in the series, as well as the size class are tabulated. The reports were analyzed to identify the number of unexpected residuals detected by intraoperative imaging, the number of cases that were re-explored following imaging, and finally, the number of cases where this led to further resection of residual adenoma. GE – general electric, NFPA – non-functioning pituitary adenoma, T – tesla, Ref – citation reference number, TSS – transsphenoidal surgery.

Data from Refs 8, 10, 11, 26–38, 40, 41, 43–55, 57–60, 63, 64, 75.